Computers and Concrete, Vol. 10, No. 4 (2012) 361-377 361
DOI: http://dx.doi.org/10.12989/cac.2012.10.4.361

Investigation of the shear behaviour of multi-story reinforced concrete walls with eccentric openings

Rafik Taleb*[1,3], Hakim Bechtoula[1], Masanubo Sakashita[2], Noureddine Bourahla[3] and Susumu Kono[2]

[1]National Center for Applied Research in Earthquake Engineering (CGS) Rue Kaddour RAHIM, BP 252, Hussein-Dey, Algiers, Algeria
[2]Departement of Architecture and Architectural Engineering, Kyoto University, Nishikyo, Kyoto 6158540, Japan
[3]Departement of Civil Engineering, Saad Dahleb Blida University, Blida, Algeria

(Received November 11, 2011, Revised March 15, 2012, Accepted April 18, 2012)

Abstract. Four Reinforced Concrete (RC) single span structural walls having various opening sizes and locations were constructed and tested under lateral reversed cyclic loading at the structural laboratory of Kyoto University. These specimens were scaled to 40% and represented the lower three stories of a six-storied RC building. The main purposes of the experimental tests were to evaluate the shear behavior and to identify the influence of opening ratios on the cracks distribution and shear strength of RC structural walls. The shear strength of the specimens was estimated by combining the shear strength of structural wall without openings and the reduction factor that takes into account the openings. Experimental and analytical results showed that the shear strength was different depending on the loading direction due to opening locations. A two-dimensional finite element analysis was carried out to simulate the performance of the tested specimens. The constructed finite elements model simulated the lateral load-drift angle relations quite well.

Keywords: multi-story RC walls; eccentric openings; static test; shear behaviour; nonlinear FEM analysis.

1. Introduction

Reinforced concrete structural walls are one of the main earthquake-resisting components for RC high-rise and mid-rise buildings. Experience from past earthquakes has shown that buildings with well-designed structural walls can significantly reduce life and economic losses (AIJ 1998, Bechtoula and Oussalem 2005). Moreover, observations from the 2010 Chile earthquake have indicated that lack of adequate detailing was the cause of several damages (Naeim *et al.* 2011). For functional reasons, the structural walls may have openings like windows, doors and duct spaces. The opening sizes, locations and shapes of openings affect their seismic performance by reducing the stiffness and the strength of the structural wall. Therefore, the design and detailing of structural walls with openings requires more attention. However, it is difficult to evaluate the shear capacity and stiffness of structural walls with openings. Evaluation is even more difficult if the openings are eccentrically located.

The structural walls with eccentric openings may be categorized as irrational shear wall structures

* Corresponding author, Ph.D., E-mail: taleb_rafik@yahoo.fr

which defy solution by normal structural analysis, and only experimental studies can disclose their behaviour (Park and Paulay 1975). During the past several decades, numerous experimental studies have been conducted on the behaviour of RC structural walls with and without openings (Ono 1995, Lopes 2001, Sakurai *et al.* 2008, Warashina *et al.* 2008, Kabeyasawa *et al.* 2009, Brun *et al.* 2011). However, the case of large and eccentric openings was not deeply investigated in the past. More experimental data are needed to clarify the shear behaviour of structural walls with eccentric openings under cyclic loading.

It is a common practice to model structural walls with openings with strut and tie models. However, the modeling procedure is not straightforward. In such cases, finite element studies may be the only alternative to understand their behaviour. Nowadays, and due to availability of powerful computers, numerical modelling approaches are able to provide an accurate alternative to the experimental investigations of reinforced concrete structural walls (Maekawa *et al.* 2003, Kim and Lee 2003, Balkaya and Kalkan 2004, Thomson *et al.* 2009, Guan *et al.* 2010).

Unlike in moment resisting buildings, where the failure mode is dominated by flexure, shear failure is usually associated with brittle failure mode with little forewarning. Therefore, the purpose of the experimental tests described herein was not only to increase the knowledge of how shear failure is critical, but also to provide a needed experimental data for further theoretical and analytical development in this area.

In the current design practice of AIJ standard (AIJ 2010), the shear strength of a structural wall with opening is estimated by applying a strength reduction factor on the strength of the structural wall without opening. The applicability of this approach is limited for opening ratio less then 0.4. The opening ratio, η, expresses the size of the opening and it is given by

$$\eta = \max\left\{\sqrt{\frac{h_0 \cdot l_0}{h \cdot l}}, \frac{l_0}{l}\right\} \tag{1}$$

Where, l is the center to center spacing between two side columns, h is the center to center spacing between the upper and lower beams and l_0 and h_0 are the length and height of the opening, respectively, as shown in Fig. 1. As it can be seen from Eq. (1), the reduction factor is independent from the opening location.

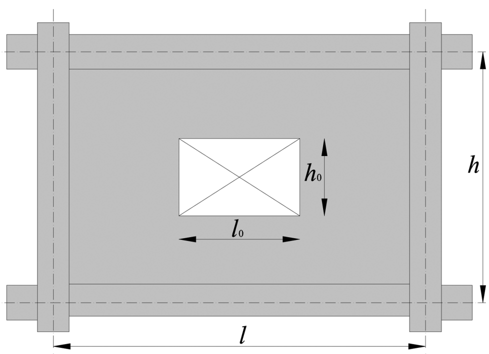

Fig. 1 Graphical representation of an opening in a structural wall

2. Experimental program

2.1 Test specimens

Four RC wall specimens were constructed and tested at Kyoto University. The specimens were three-storied and 40% scaled models. As shown in Fig. 2, three of these specimens ($S1$, $M1$, $L1$) were with eccentric openings and one specimen ($N1$) without openings. For specimens with openings, the main test variables were the opening ratio and the opening location. The main purposes of the experimental tests were to evaluate the shear behavior and to clarify the influence of opening ratios on the cracks distribution and the shear strength of structural walls under horizontal reversed cyclic loading. The opening ratios were 0.3, 0.34 and 0.46 for $S1$, $M1$ and $L1$ specimen, respectively. All the specimens were 4150 mm height and 2800 mm wide. The beams were nominally 200 mm wide by 300 mm deep and the side columns were 300 mm by 300 mm. The thickness of wall panels was 80 mm. To provide a fixed base at the bottom, a RC foundation beam with 600 mm wide by 400 mm thick and 3600 mm in length was built integrally with the body of the structural walls and post-tensioned to the reaction floor prior to testing. The clear span was 2200 mm and the column clear story height was 1100 mm, 1100 mm and 550 mm in the first,

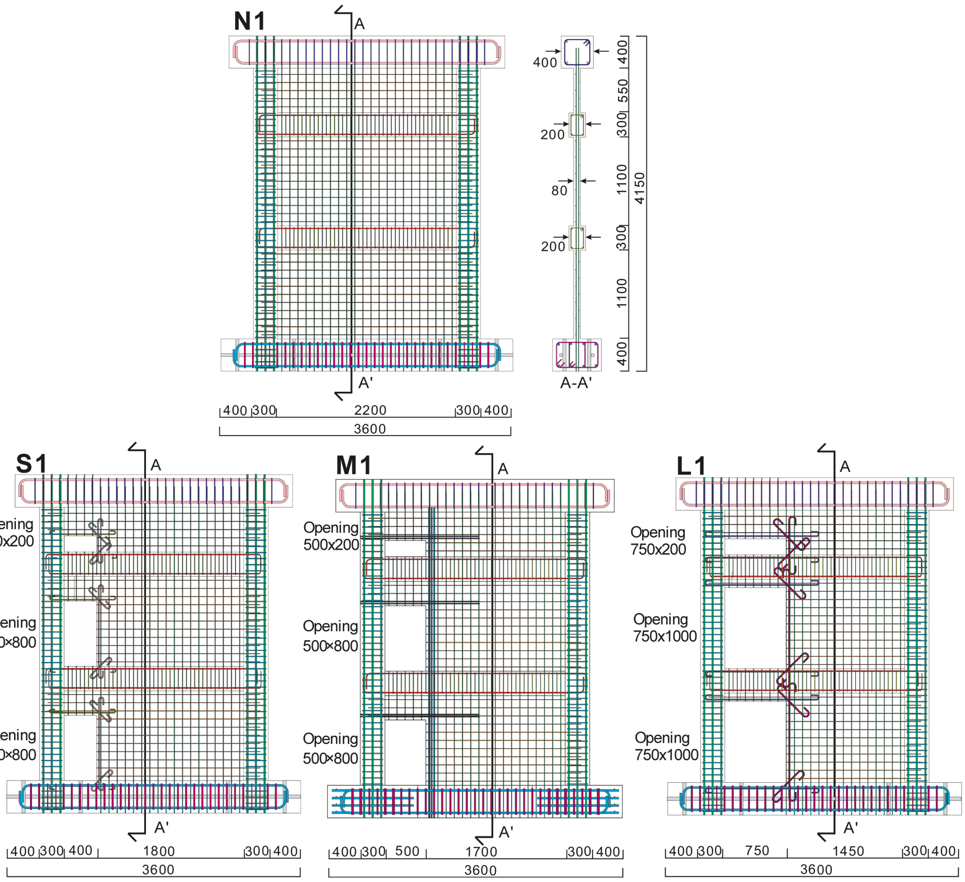

Fig. 2 Specimen configurations and reinforcing bars arrangement

second and third story, respectively.

A 400 mm wide by 400 mm deep loading beam was cast at the top of the wall panel. A hydraulic actuator was attached to the specimen at mid-span of the loading beam to apply the horizontal reversed cyclic loading. The third story was provided for releasing the confinement caused by the stiff loading beam at the top. The structural walls were tested in a lateral reverse cyclic manner until their maximum performances. Since one of the purposes of this study is to clarify the influence of the opening ratios on the shear behaviour, all the specimens were designed to fail in shear and not in flexure.

2.2 Material properties

Table 1 shows the cross section dimensions and the reinforcement arrangement. Typical beam section was composed of two $D13$ bars for top and bottom reinforcement, with $D6$ closed stirrups spaced at 100 mm. The side column section contained eight $D19$ bars, with $\phi10$ closed stirrups spaced at 75 mm. The foundation beam section contained four $D25$ bars as top and bottom reinforcement, with $D10$ double closed stirrups spaced at 100 mm. The loading beam section contained two $D25$ bars as top and bottom reinforcement with $D10$ closed stirrups spaced at

Table 1 Cross section dimension and reinforcement arrangement

Element	Beam	Column	Wall	Loading beam	Foundation
Section (mm)	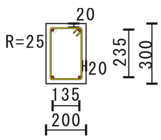	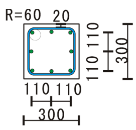	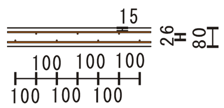	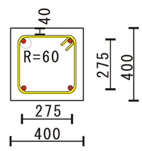	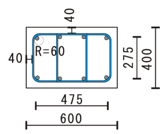
Dimension	200×300	300×300	Thickness 80	400×400	400×600
Main bar	2-$D13$	8-$D19$	Vertical: $D6$@100	4-$D25$	8-$D25$
Stirrup	2-$D6$@100	2-$\phi10$@75	Horizontal: $D6$@100	2-$D10$@100	4-$D10$@100

Table 2 Reinforcing bars around opening

Specimen	Opening ratio	Vertical reinforcing	Horizontal reinforcing	Diagonal reinforcing
$S1$	0.30	1-$D13$	2-$D10$	1-$D13$
$M1$	0.34	3-$D13$	3-$D10$	-
$L1$	0.46	1-$D16$	2-$D13$	1-$D16$

Table 3 Concrete material properties

Specimen	Compressive strength (MPa)	Tensile strength (MPa)	Young's modulus (GPa)
$N1$	25.9	2.3	21.0
$S1$	25.1	2.2	21.7
$M1$	21.7	2.1	15.8
$L1$	28.9	2.5	26.0

Table 4 Reinforcements properties

Nominal diameter	Yield strength (MPa)	Maximum strength (MPa)	Young's modulus (GPa)
*D*6	425	538	204
*D*10	352	496	186
*D*13	362	529	188
*D*19	411	605	189
*D*25	387	541	194
ϕ10	1033	1221	204

100 mm. Table 2 shows the reinforcing bars around openings as well as the opening ratios. Material properties of concrete and reinforcement adopted for the specimens are listed in Tables 3 and 4, respectively.

2.3 Experimental setup and testing procedure

Figs. 3 and 4 show the experimental setup and the details of loading system, respectively. The lateral load, Q, was applied statically to the loading beam by two 2 MN hydraulic jacks. Cyclic reversed horizontal loads were statically applied to the specimens in both positive and negative directions. During the cyclic horizontal loading, vertical axial loads were applied to columns by two 1 MN hydraulic jacks assuming that the specimens are representing the lower three stories of a typical six stories RC building. The vertical axial load levels were determined in accordance with the assumed long-term axial loads for a six-story wall with three spans. As an initial condition and

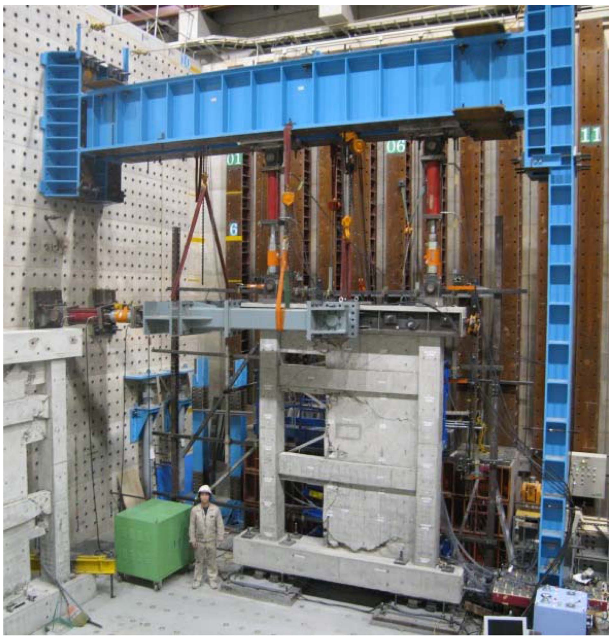

Fig. 3 Test setup

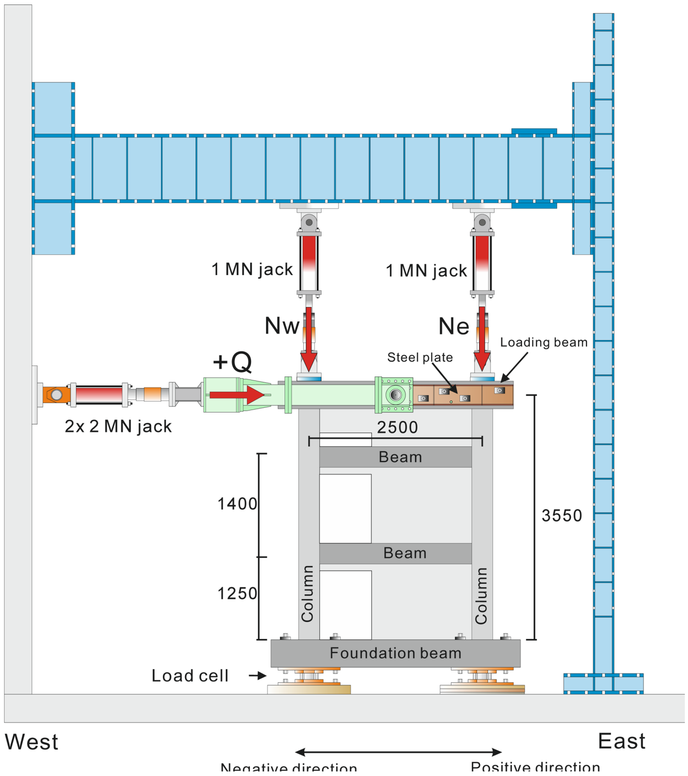

Fig. 4 Loading system

for each vertical jack, a 400 kN axial load was applied representing the effect of the upper stories. The two vertical hydraulic jacks were adjusted to apply two vertical forces, *Nw* and *Ne*, that vary as a function of the applied lateral load, Q, in order to keep the shear span ratio (M/Ql) equal to 1.0, where, M is the flexural moment applied at the base of the wall, Q is the horizontal load applied to the loading beam and l is the distance between the center to center of the two side columns. This will insure that the shear damages in the wall will precede the flexural yielding of the wall. The influence of the axial load level on the shear capacity of each wall was insignificant since the side columns were not damaged until the end of the tests. Loading was mainly controlled by measured displacement in terms of the story drift angle. The same loading history was used to test all specimens. The loading history was divided into two parts: The first cycle of loading was performed up to 200 kN, after that, two cycles of repeated loading were applied for each drift angle, R, of ±0.05, ±0.1, ±0.25, ±0.5, ±0.75, ±1.00 and ±1.5%.

Instrumentation was set on the specimens to monitor the deformations on the elements and strains in the reinforcements. At each peak of the loading history, cracks widths were measured and damages to the specimens were photographed. Crack location, spalling of concrete and location of any buckled steel reinforcements bars were reported. Each test was carried out until the specimen experienced a significant loss of shear capacity.

3. Interpretation of experimental results

3.1 Damages and crack pattern

Fig. 5 shows the crack patterns observed on specimen $N1$, $S1$, $M1$ and $L1$ at the drift angle of 0.75%. Figs. 6 to 9 show the crack propagation at the end of tests for specimen $N1$, $S1$, $M1$ and $L1$, respectively. For all specimens, the cracking started with the apparition of diagonal cracks in the wall panels at the upper part of the openings at 0.05% drift angle. Flexural cracks in the tensile side column were also observed. As the applied drift angle increased, the number of shear cracks increased in the wall panels and showed a downward trend illustrating the stress transfer path. For specimens with opening, the formation of a shear transfer truss mechanism was prevented, and the shear stress trended to concentrate at the bottom corner of the openings. When the drift angle increased from 0.5% to 0.75%, the lateral load reached its maximum. Excessive damage was observed after reaching the peak load. At this stage, some longitudinal bars of the beams and reinforcement of the wall were exposed due to the spalling of cover concrete, and buckling of some of the wall reinforcement at the first story were observed. At the final loading stage, the shear

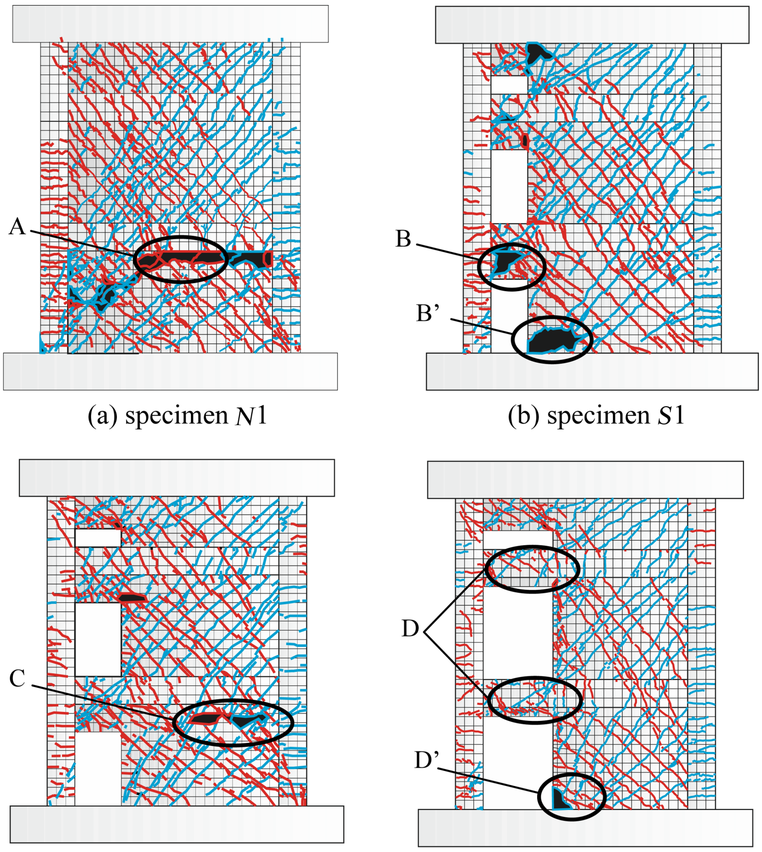

(a) specimen $N1$ (b) specimen $S1$

(c) specimen $M1$ (d) specimen $L1$

Fig. 5 Crack pattern at 0.75% drift angle sliding of the wall occurred, and the residual strength decreased significantly. The above mentioned cracking progress was common to the four specimens. Hereafter, specific details of the observed damages are given for each specimen.

Specimen *N*1: Shear cracks were observed at the wall panels and at the second story short-span beam at +0.05% drift angle. At the drift angle of +0.1%, flexural cracks were observed in the tensile side column of the first story. At +0.5% drift angle, spalling of concrete at the boundary between wall panel and beam of the first story occurred; while, severe damage was observed at the base of the compression side column of the first story. At the drift angle of +0.75%, shear sliding occurred at the top of the first story wall panel, location A in Fig. 5(a), followed by sudden strength degradation.

Specimen *S*1: Shear cracks at the first story wall panel and flexural cracks in the tensile side column were observed at the drift angle of +0.05%. Shear cracks propagated furthermore in the wall panels and progressed to the beams at 0.1% drift angle. At the drift angle of -0.5%, concrete at the corner of the opening in the first story was severely damaged as illustrated in Fig. 5(b) location B. Spalling of concrete at the first story wall and the second story short span beam was also observed. Buckling of the vertical reinforcements near the opening took place at the first story wall panel at the drift angle of -0.75%, see location B' in Fig. 5(b). At -1.0% drift angle, shear sliding occurred at the bottom of the first story wall.

Specimen *M*1: Shear cracks in the wall panels and flexural cracks in the tension side of the first story column were observed at the drift angle of ±0.05%. At -0.25% drift angle, shear cracks occurred in the short span beam of the second story. Spalling of cover concrete at the first story wall occurred at drift angle of -0.5%, shown in Fig. 5(c) by location C. Observed damage for specimen *M*1 was slighter than that of specimen *S*1. However, shear cracks were more important than those of specimen *L*1. At the drift angle of -0.75%, shear sliding occurred in the wall at the first story.

Specimen *L*1: shear cracks at the first story wall and flexural cracks in the tensile side column were observed at the drift angle of +0.04% like for the case of specimen *S*1. However, cracks of the short span beam at the second and the third story (location D in Fig. 5(d)) were not important as those observed for specimen *S*1. This difference is due to the difference in the length of beams. At drift angle of -0.5%, buckling of longitudinal reinforcement around the opening of the first story took place and severe damage of concrete was observed at -0.75 drift angle, and showed by location D' in Fig. 5(d). At the drift angle of +1.5%, shear sliding occurred in the wall of the first story. The lateral reinforcing bars of the first story wall panel were bent severely, and cracks have propagated extensively along the wall reinforcements. For this specimen, *L*1, the strength degradation after the peak load did not drop suddenly like observed for the case of specimens *S*1 and *M*1.

3.2 Lateral load-drift angle relation

Figs. 6 to 9 show the hysteresis curves of the lateral load versus the drift angle for specimen *N*1, *S*1, *M*1 and *L*1, respectively. Table 5 summarizes the maximum lateral load and the corresponding drift angle. It can be seen that the maximum shear strength of specimen *L*1 is the lowest one among the other specimens, either in positive loading direction or in negative loading direction, due to the fact that this specimen has the largest opening ratio. It can be noted also that, the maximum strength attained during the positive loading direction is larger than that reached during the negative loading direction due to the eccentric opening location and the shear transfer mechanism. These results

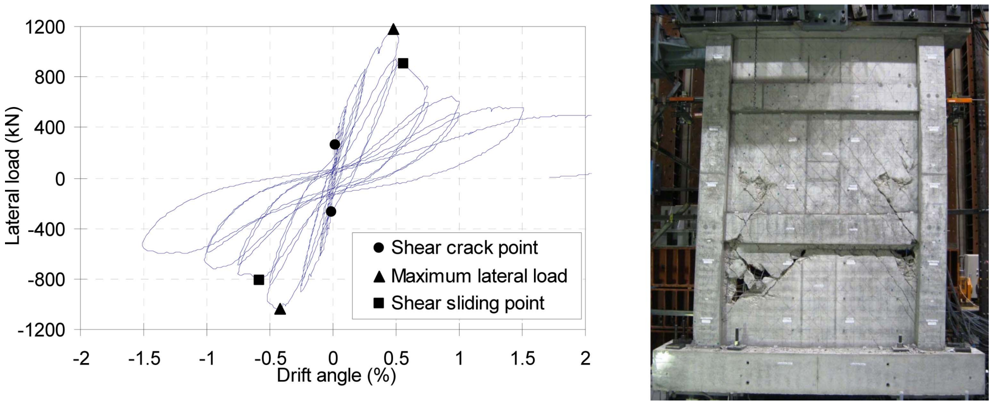

Fig. 6 Hysteresis curve and observed damage at the end of test - specimen *N*1-

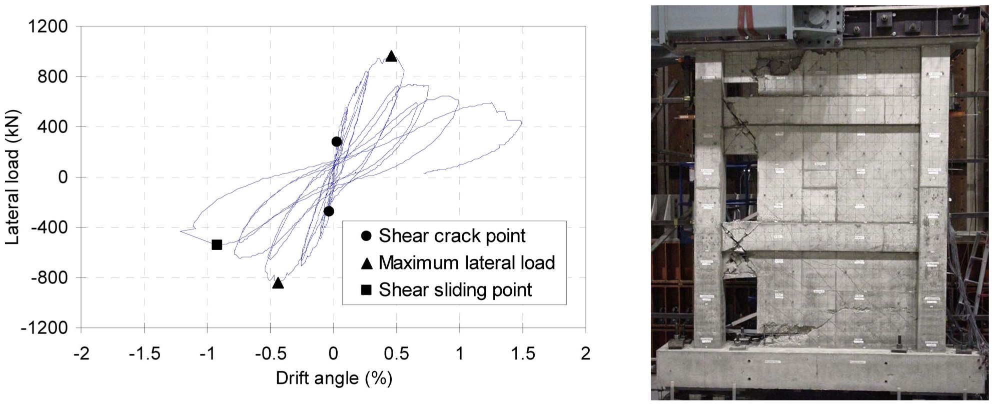

Fig. 7 Hysteresis curve and observed damage at the end of test - specimen *S*1-

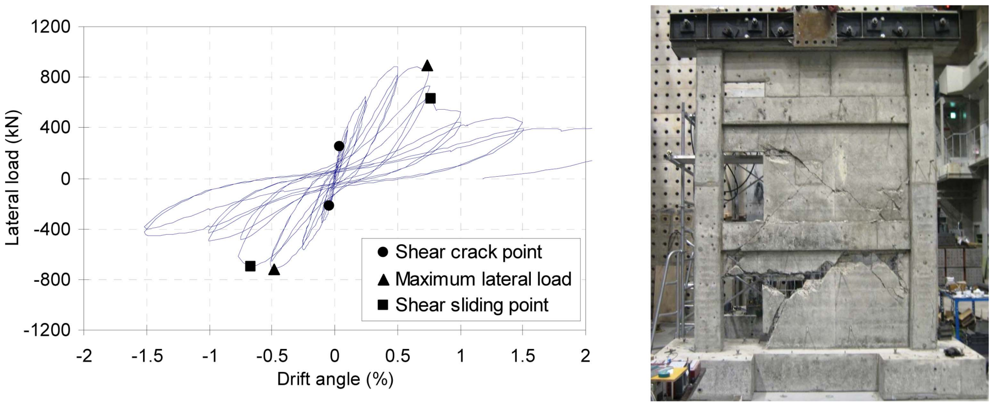

Fig. 8 Hysteresis curve and observed damage at the end of test - specimen *M*1-

emphasise the importance of the loading direction. The strength degradation after the peak load was more pronounced for specimens *S*1 and *M*1 than the others.

With respect to the failure mode, both specimens *S*1 and *M*1 failed in a brittle manner after

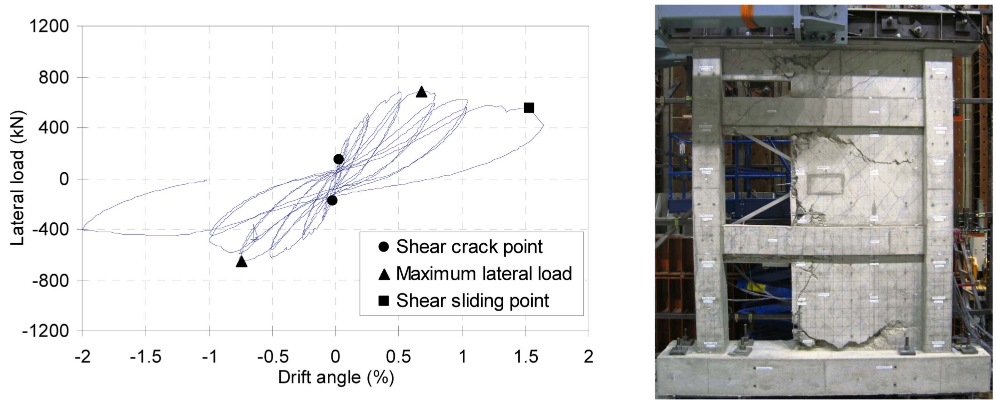

Fig. 9 Hysteresis curve and observed damage at the end of test - specimen *L*1-

Table 5 Maximum lateral loads and corresponding drift angles

	Positive direction		Negative direction	
	Maximum load (kN)	Drift angle (%)	Maximum load (kN)	Drift angle (%)
*N*1	1179	0.48	-1039	-0.42
*S*1	967	0.46	-838	-0.44
*M*1	889	0.74	-723	-0.48
*L*1	686	0.68	-649	-0.74

reaching the peak load. Specimen *S*1 failed by shear failure of the short span beams, while *M*1 failed by shear sliding at the first story wall panel. On the other hand, *L*1 failed in a ductile manner after flexural yielding of the short span beam took place followed by shear sliding of the wall panel at the final stage.

For all specimens, main reinforcements of side columns at the bottom of the first story yielded at the drift angle of about 1.0%, while those of short span beams yielded at the drift angle of about 0.25%. All stirrups of the short span beams of *S*1 and *M*1 yielded, while those of short span beam of *L*1 yielded at the first story only. Most of the lateral reinforcements of wall panel yielded around the peak load corresponding to the drift angle of about 0.5%. For walls with openings, most of the reinforcing bars around the openings were yielded at the drift angle of about 1.0%.

4. Prediction of the shear strength

A simple method was used to estimate the shear strength, Q_{su}, of a structural wall with openings based on shear strength of a structural wall without openings which is given by

$$Q_{su} = r_u \cdot V_u \tag{2}$$

Where, r_u is the shear strength reduction factor and V_u is the shear strength of a structural wall without openings.

4.1 Shear strength reduction factor of AIJ standard

In the design practice of the Architectural Institute of Japan standard (AIJ 2010), the strength reduction factor, r_u, adopted to calculate the shear strength of a structural wall with openings was defined as follow

$$r_u = \min(r_1, r_2, r_3) \tag{3}$$

Where

$$r_1 = 1 - 1.1\frac{l_0}{l} \tag{4}$$

$$r_2 = 1 - 1.1\sqrt{\frac{h_0.l_0}{h.l}} \tag{5}$$

$$r_3 = 1 - \frac{1}{2}\left(1 + \frac{l_0}{l}\right)\frac{h_0}{h} \tag{6}$$

With

$$\lambda = \frac{1}{2}\left(1 + \frac{l_0}{l}\right) \tag{7}$$

All the parameters of the above equations were already defined in Section 1. The maximum opening ratio is limited to 0.4 in the AIJ standard when the wall strength reduction factor due to openings is determined based on the shear strength of a structural wall without openings.

4.2 Ono's shear strength reduction factor

Considering the effective diagonal compression field of the concrete panel, as shown in Fig. 10, strength reduction factor, r_u, was proposed by Ono (Ono and Tokuhiro 1992, Ono 1995) as follow

$$r_u = \sqrt{\frac{\sum A_e}{h.l}} \tag{8}$$

Where, A_e is the area of the effective diagonal compression field, h is the distance between the upper and lower beams and l is the distance between the two boundary columns. Ono's strength reduction factor takes into account the opening location as well as opening dimensions. For multi-

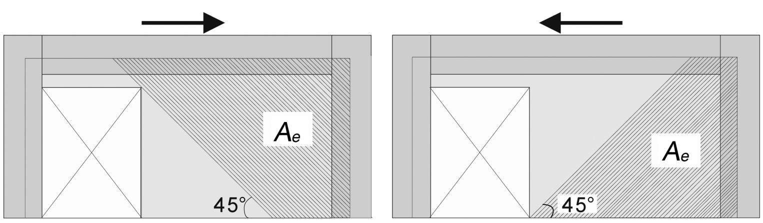

(a) Positive loading (b) Negative loading

Fig. 10 Area of the wall panel forming a compression field story wall with openings, Ono's reduction factor is taken as the minimum of Ono's reduction factor of each story.

4.3 Shear strength of structural wall without openings

In this study, two methods were used to estimate the shear strength, V_u, of a structural wall without openings. The first method is based on truss and arch mechanism given by (AIJ 2004)

$$V_u = t_w l_{wb} p_s \sigma_{sy} \cot\phi + \tan\theta (1-\beta) t_w l_{wa} \nu \sigma_B / 2 \tag{9}$$

With

$$\tan\theta = \sqrt{[(h_w/l_{wa})^2 - 1]} - h_w/l_{wa} \tag{10}$$

$$\beta = (1-\cot^2\phi) p_s \sigma_{sy} / (\nu \sigma_B) \tag{11}$$

Where, t_w is the thickness of the wall panel, h_w is the height of the wall, l_{wb} and l_{wa} are the equivalent lengths of the wall panel in the truss mechanism and arch mechanism, respectively, σ_B is the compressive strength of concrete, σ_{sy} is the yield strength of the shear reinforcement within the wall panel, p_s is the shear reinforcement ratio within the wall panel, ϕ is the angle of the compressive strut in the truss mechanism and ν is the effectiveness factor for the compressive strength of concrete.

The second method is based on Arakawa's equation given by (JBDPA 2001)

$$V_u = \left[\frac{0.053 p_{te}^{0.23} (17.6 + F_c)}{M/(Q.l) + 0.12} + 0.845 \sqrt{p_{se} \cdot \sigma_{wy}} + 0.1 \sigma_{0e} \right] \cdot b_e \cdot j_e \tag{12}$$

Where, p_{te} is the equivalent tensile reinforcement ratio, F_c is the concrete compressive strength, (M/Ql) is the shear span ratio, p_{se} is the transversal equivalence ratio, σ_{wy} is the yield strength of the transversal reinforcement, σ_{0e} is the axial stress, b_e is the equivalent wall thickness and j_e is the stress center distance.

4.4 Results of the shear strength prediction

Comparison of the calculated shear strengths using the mentioned methods given by Eqs. (9) and (12) to the experimental results is summarized in Tables 6 and 7, respectively. In these two tables, Q_{Exp}, Q_{AIJ}, Q_{Ono} are the shear strength obtained from the test, using the AIJ standard reduction factor and the Ono's reduction factor, respectively. Arakawa's equation gives conservative values of shear strength because the formula is based on lower limit of shear strength. Shear strength prediction based on truss and arch mechanism agreed well with the experimental values of shear strength. Using truss and arch mechanism equation, shear strength calculated using AIJ's reduction factor agree well with the experimental results in negative direction. While in the positive direction, the shear strength is underestimated. This difference is due to the fact that AIJ's reduction factor is the same in the positive and negative loading direction and does not reflect the opening position. Ono's reduction factor method gave a better estimation of the shear strength either in positive and negative loading direction, because the effective area of wall corresponding to the compressive field in positive direction and negative direction was taken into account.

Table 6 Comparison of the shear strengths using Eq. (9)

	Positive direction			Negative direction		
	Q_{Exp} (kN)	Q_{AIJ} (kN)	Q_{Ono} (kN)	Q_{Exp} (kN)	Q_{AIJ} (kN)	Q_{Ono} (kN)
$N1$	1179	1120(1.05)		-1039	-1120(0.93)	
$S1$	967	750(1.29)	941(1.03)	-838	-750(1.12)	-862(0.97)
$M1$	889	728(1.22)	918(0.97)	-723	-728(0.99)	-829(0.87)
$L1$	686	582(1.18)	784(0.88)	-649	-582(1.12)	-717(0.91)

The value in ( ) is the ratio between the experimental value to the calculated value.

Table 7 Comparison of the shear strengths using Eq. (12)

	Positive direction			Negative direction		
	Q_{Exp} (kN)	Q_{AIJ} (kN)	Q_{Ono} (kN)	Q_{Exp} (kN)	Q_{AIJ} (kN)	Q_{Ono} (kN)
$N1$	1179	854(1.38)		-1039	-854(1.22)	
$S1$	967	593(1.63)	717(1.35)	-838	-593(1.41)	-658(1.27)
$M1$	889	506(1.76)	700(1.27)	-723	-506(1.43)	-632(1.14)
$L1$	686	461(1.49)	598(1.15)	-649	-461(1.41)	-547(1.19)

The value in ( ) is the ratio between the experimental value to the calculated value.

5. Nonlinear FEM analysis

5.1 Analytical model

A two-dimensional static nonlinear FEM analysis was carried out for all specimens. The validity of analytical model is examined to investigate the stress transfer mechanism of RC shear wall with eccentric openings. The finite element mesh for specimen $S1$ is shown in Fig. 11. The element size of

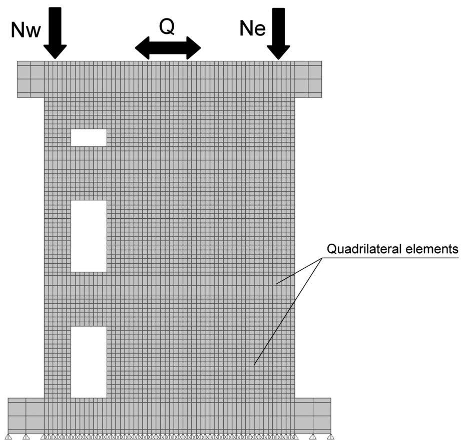

Fig. 11 Finite element mesh (specimen $S1$)

the mesh in the wall panels was 50×50 mm. Each node at the bottom of the foundation beam had pin support to restrain vertical and lateral displacement. Loading beam and foundation beam were assumed to be elastic. Horizontal and vertical reinforcement was smeared assuming a perfect bond but diagonal reinforcement was neglected. The FEM non-linear analysis software FINAL was used in this analysis.

5.2 Element model

Mechanical properties of material model used in the analysis are thus given in Tables 3 and 4. Quadrilateral plane stress elements were used for concrete. Reinforcing bars were substituted equivalent layers with stiffness in the bar direction and superposed on the quadrilateral elements assuming a perfect bond. For reinforcing bars material, the von Mises yield surface is employed to judge yielding under a multi-axial stress field along with the associated flow rule for isotropic hardening. The stress-strain relationship follows Ciampi's model (Ciampi *et al.* 1982). As for the stress-strain relationship of concrete, a modified Ahmad model was adopted for the compressive stress-strain curve (Ahmad and Shah 1982). The model by Kupfer and Gerstle (1973) was adopted as the fracture criterion of concrete under biaxial stress state, and the compressive strength reduction factor was adopted from Naganuma (Naganuma 1991). The concrete tension stiffing model and the shear transfer model after cracks proposed by Naganuma was adopted (Naganuma and Ohkubo 2000).

5.3 Analysis results

Analytical lateral load-drift angle relations are compared with the experimental results in Fig. 12.

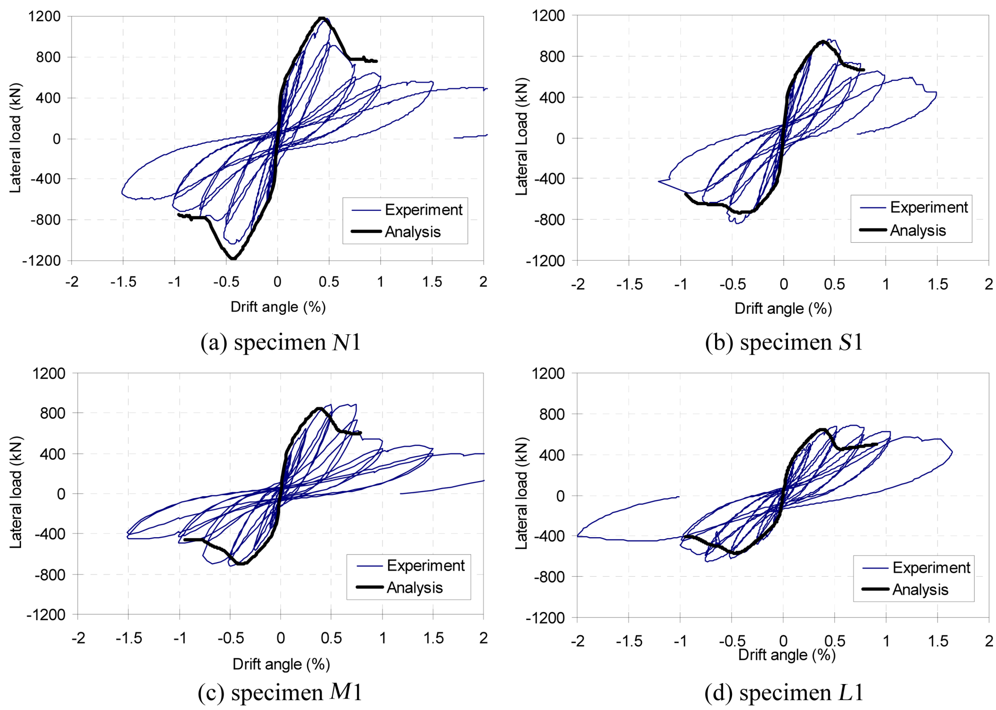

Fig. 12 Lateral load-drift angle relationships

Table 8 Comparison of the maximum lateral loads

	Positive direction					Negative direction				
	Maximum load (kN)			Drift angle (%)		Maximum load (kN)			Drift angle (%)	
	Q_{Exp}	Q_{FEM}	Q_{Exp}/Q_{FEM}	R_{Exp}	R_{FEM}	Q_{Exp}	Q_{FEM}	Q_{Exp}/Q_{FEM}	R_{Exp}	R_{FEM}
*N*1	1179	1183	1.00	0.48	0.44	-1039	-1183	0.88	-0.42	-0.44
*S*1	967	940	1.03	0.46	0.40	-838	-732	1.14	-0.44	-0.43
*M*1	889	850	1.05	0.74	0.38	-723	-651	1.11	-0.48	-0.40
*L*1	686	649	1.06	0.68	0.38	-649	-573	1.13	-0.74	-0.46

Table 7 shows a comparison between the experimental and the FEM peak loads with the corresponding drift angle. The analytical envelop curves matched well with the experimental results for all specimens as illustrated in Fig. 12. The FEM peak loads agreed well with the experimental ones. As for the corresponding drift angle, a good agreement is observed for specimens *N*1 and *S*1, while for specimens *M*1 and *L*1, with larger opening ratio, the model underestimate this value. This can be explained by the fact that, for specimens with large openings, the flexural component became more important than in the case of specimens with small openings.

6. Conclusions

Cyclic loading tests were conducted on four 40%-scale specimens in order to evaluate the shear behaviour of RC structural walls with eccentric openings. The specimens represented the lower three stories of a six-story reinforced concrete building. The following conclusions can be drawn.

- Shear strength of a structural wall was different between positive and negative loading directions due to the eccentric opening location. Shear strength obtained while loading from the opening side was larger than that obtained from the opposite side. The raison was due to the existence of eccentric openings that affected the formation of concrete strut. Shear transfer mechanism was interrupted and the concrete damage at the corner of the opening caused the sliding failure of wall. It is recommended that this phenomenon should be assessed carefully through other tests and should be taken into account in the future design standard.
- Shear strength of specimen *S*1 with small opening ratio was higher than those of specimens *M*1 and *L*1 with larger opening ratio. However, specimen *S*1 showed a sudden drop of its performance due to the existence of short span beams that yielded at the early loading stage. Specimen *L*1 showed a smooth decrease of the strength after the peak load in a ductile manner. Opening ratios affect the shear strength especially when the openings of the structural walls are at the same location.
- Since Ono's reduction factor method considered the effective concrete compressive field of the structural wall, the calculated shear strengths using this method agreed well with the experimental ones and at the same time confirmed the shear transfer mechanism. It is worth to mention that, damage to the compressed concrete of the first story wall, was the principal factor which influenced the shear capacity of the multi-story structural walls.
- In order to simulate the behavior of the specimens, a nonlinear static finite elements analysis was carried out using a two-dimensional model. The analysis gave a good agreement for the maximum peak loads and corresponding drift angles.

Acknowledgements

The reported research herein was supported by the grants from the Grants-in-Aid for Scientific Research of Japan (No. 16206056), which is gratefully acknowledged. The authors would like also to thank the graduate students M. Warashina, K. Mori, M. Doi and K. Chosa for their great assistance and help during the experiments and the data process.

References

Ahmad, S.H. and Shah, S.P. (1982), "Complete triaxial stress-strain curve for concrete", *ASCE J. Struct. Div.*, **108**(4), 728-742.

Architectural Institute of Japan (2010), *AIJ Standard for structural calculation of reinforced concrete structures (Revised 2010)*, Architectural Institute of Japan, Tokyo, Japan.

Architectural Institute of Japan (2004), *Guidelines for performance evaluation of earthquake resistant reinforced concrete buildings*, Architectural Institute of Japan, Tokyo, Japan.

Architectural Institute of Japan (1998), *Report on the Hanshin-Awaji earthquake disaster building series Volume 1: Structural damage to reinforced concrete building*, Architecture Institute of Japan, Tokyo, Japan.

Balkaya, C. and Kalkan, E. (2004), "Three-dimensional effects on openings of laterally loaded pierced shear walls", *J. Struct. Eng.-ASCE,* **130**(10), 1506-1514.

Bechtoula, H. and Ousalem, H. (2005), "The 21 May 2003 Zemmouri (Algeria) Earthquake: Damages and disaster responses", *J. Adv. Concr. Techno.*, **3**(1) 161-174.

Brun, M., Labbe, P., Bertrand, D. and Courtois, A. (2011), "Pseudo-dynamic tests on low-rise shear walls and simplified model based on the structural frequency drift", *Eng. Struct.*, **33**(3), 796-812.

Ciampi, V., Eligehausen, R., Bertero, V.V. and Popov, E.P. (1982), *Analytical model for concrete anchorages of reinforcing bars under generalized excitations*, Report No. UCB/EERC 82-23, Earthquake Engineering Research Center, University of California, Berkeley, California.

FINAL/99, *Finite elements analysis program for the nonlinear behaviour of concrete structures*, ITOCHU Techno-Solutions Corporation.

Guan, H., Cooper, C. and Lee, D.J. (2010), "Ultimate strength analysis of normal and high strength concrete wall panels with varying opening configurations", *Eng. Struct.*, **32**(5), 1341-1355.

Japan Building Disaster Prevention Association (2001), *Standard for seismic evaluation of existing reinforced concrete buildings*, Japan Building Disaster Prevention Association, Tokyo, Japan.

Kabeyasawa, T., Kabeyasawa, T., Kim, Y., Kabeyasawa, T. and Bae, K. (2009), *Tests on reinforced concrete columns with wing walls for hyper-earthquake resistant system*, 3rd International Conference on Advances in Experimental Structural Engineering, San Francisco, USA.

Kabeyasawa, T., Kim, Y., Sato, M., Hyunseong, H. and Hosokawa, Y. (2011), "Tests and analysis on flexural deformability of reinforced concrete columns with wing walls", *Proceedings of the 9th Pacific Conference on Earthquake Engineering Building an Earthquake-Resilient Society*, Auckland, New Zealand.

Kim, H.S. and Lee, D.G. (2003), "Analysis of shear wall with openings using super elements", *Eng. Struct.*, **25**(8), 981-991.

Kupfer, H.B. and Gerstle, K.H. (1973), "Behavior of concrete under biaxial stress", *J. Eng. Mech.-ASCE,* **99**(4), 853-866.

Lopes, M.S. (2001), "Experimental shear-dominated response of RC walls. Part II: Discussion of results and design implications", *Eng. Struct.*, **23**(5), 564-574.

Maekawa, K., Pimanmas, A. and Okamura, H. (2003), *Nonlinear mechanics of reinforced concrete*, Spon Press, London.

Miao, Z.W., Lu, X.Z., Jiang, J.J. and Ye, L.P. (2006), "Nonlinear FE model for rc shear walls based on multi-layer shell element and microplane constitutive model", *Proc. Computational Methods in Engineering And Science (EPMESC X)*, Tsinghua University Press & Springer-Verlag, China.

Naeim, F., Lew, M., Carpenter, L.D., Youssef, N.F., Rojas, F., Saragoni, G.R. and Adaros, M.S. (2011), "Performance of tall buildings in Santiago, Chile during the 27 February 2010 offshore Maule, Chile earthquake", *Struct. Des. Tall Spec.*, **20**(1), 1-16.

Naganuma, K. (1991), "Nonlinear analytical model for reinforced concrete panels under in-plane stresses", *J. Struct. Constr. Eng.*, 421, 39-48.

Naganuma, K. and Ohkubo, M. (2000), "An analytical model for reinforced concrete panels under cyclic stresses", *J. Struct. Constr. Eng.*, 536, 135-142.

Ono, M. (1995), "Experimental study on reinforced concrete opening wall above opening periphery ratio 0.4, Part1~Part2", *Summaries of Technical Papers of Annual Meeting of Architectural Institute of Japan* C-2, Structures IV: 147-150.

Ono, M. and Tokuhiro, I. (1992), "A proposal of reducing rate for strength due to opening effect of reinforced concrete framed shear walls", *J. Struct. Constr. Eng.*, 435, 119-129.

Park, R. and Paulay, T. (1975), *Reinforced concrete structures*, John Wiley & Sons, New York.

Sakurai, M., Kuramoto, H., Matsui, T. and Akita, T. (2008), "Seismic performance of RC shear walls with multi-openings", *Proceeding of 14th Word Conference on Earthquake Engineering (14WCEE)*, Beijing, China.

Thomson, E.D., Perdomo, M.E., Picón, R., Marante, M.E. and Flórez-López, J. (2009), "Simplified model for damage in squat RC shear walls", *Eng. Struct.*, **31**(10), 2215-2223.

Warashina, M., Kono, S., Sakashita, M. and Tanaka, T. (2008), "Shear behaviour of multi-story RC structural walls with eccentric openings", *Proceeding of 14th Word Conference on Earthquake Engineering (14WCEE)*, Beijing, China.

CC